

Development of real-time muscle stiffness sensor based on resonance frequency for physical Human Robot Interactions

Hyonyoung Han, Heeseop Han and Jung Kim, *Member, IEEE*

Abstract— This paper presents a new type of muscle contraction sensor for motion intention detection algorithm in physical human robot interaction (pHRI). The resonance frequency shift by muscle contraction was measured by piezoelectric material. The developed sensor can measure muscle activations accurately over clothes and this is an advantage over the conventional surface Electromyography (sEMG). Performances of the sensor are evaluated through isometric wrist flexion motion tests based on maximal voluntary contraction (MVC) in two aspects: accuracy and speed. While the flexor carpi radialis (FCR) contraction tests up to 40% MVC, sensor outputs are compared with force sensor outputs. The result shows that we can measure muscle contraction by the developed sensor with high correlation and fast response, which is desirable for many physical human robot interactions including exoskeleton devices.

I. INTRODUCTION

Motion estimation of the human limb is a challenging issue in physical human-robot interaction (pHRI) [1, 2]. The estimation can be applied to support intuitively controllable prosthesis for limb amputees and enhance physical strength for the elderly. The motion estimation is generally classified into three steps [3, 4]: information sensing, intention understanding, and device control. Among the steps, we are interested in the information sensing, that acquires motion information from the limb kinematic data, limb kinetic data, and bioelectrical activity data [5]. Researchers study the bioelectrical activity data for estimation of the motions to reduce the electromechanical delay [6, 7]. The surface electromyography (sEMG) is a widely used bioelectrical activity data [9, 10] which is a neuromuscular signal for muscle activation, but it has following limitations: sensitivity according to attachment sites, skin conditions, and electromagnetic noises. Moreover, the sEMG requires direct contact to the skin, making the attachment uncomfortable. To overcome the limitations of the sEMG, researchers are interested in the biosignal sensors that measure the

physiological and physical changes of the skeletal muscle during the contraction. Mechanomyography (MMG) is muscle vibration signal due to lateral movement of muscle fibres [11, 12]. The MMG is more robust to attachment location and skin condition than sEMG, yet motion artifacts limit the accuracy. Other biosignal sensors based on muscle properties are also being developed: optical density [13], elastography [14], length change [15], pressure [16], myokinematic (MK) muscle expansion [17, 18], and stiffness [19, 20]. However, the optical density sensor requires direct contact to the skin, and other sensors have limitations in measurement difficulties in fine muscles.

In this paper, we develop a real-time muscle contraction sensor, namely active muscle stiffness sensor (aMSS), based on muscle resonance frequency. The sensor measures the muscle contraction from the stiffness actively by generating and sensing resonance vibrations using piezoelectric transducers. As muscle becomes stiffer, the resonance frequency becomes larger [21]. The sensor can measure the muscle contraction over clothes without contacting the skin directly, and this is a strong advantage of this new type sensor.

II. BACKGROUND

A. Principles of resonance-based stiffness sensor

Materials have typical frequency characteristics called resonance, which is a tendency to oscillate at certain frequency. A material's resonance frequency depends on its stiffness as well as mass. As the material becomes stiffer, the resonance frequency also becomes higher.

In this study, the piezoelectric resonating probe was used to generate oscillation and measure associated changes in signals by muscle contractions. Because PZTs have both electrical and mechanical characteristics, we must analyze the response by considering the mechanical properties and the electrical impedance. The frequency shift (Δf_r) of the PZT (1) is related to the impedance of the object in contact [21],

$$\Delta f_r = -\frac{\sqrt{k/\rho}}{2\pi l} \times \frac{m\omega - \frac{k}{\omega}}{Z_{PZT}} \quad (1)$$

where ρ , l , Z_{PZT} are density, length and impedance of the PZT, and ω , m and k are the oscillation frequencies, mass and stiffness of the muscle containing tissues, respectively.

This research was supported by the Happy tech. program through the National Research Foundation of Korea(NRF) funded by the Ministry of Education, Science and Technology (No. 2011-0020934).

H. Han is with the Department of Mechanical Engineering, Korea Advanced Institute of Science and Technology (KAIST), Daejeon, 305-701, Korea (e-mail: hhn98@kaist.ac.kr).

H. Han is with the Department of Mechanical Engineering, Korea Advanced Institute of Science and Technology (KAIST), Daejeon, 305-701, Korea (e-mail: hhseop@kaist.ac.kr).

J. Kim is with the Department of Mechanical Engineering, Korea Advanced Institute of Science and Technology (KAIST), Daejeon, 305-701, Korea (phone:+82-42-350-3231; fax: +82-42-350-5230; e-mail: jungkim@kaist.ac.kr).

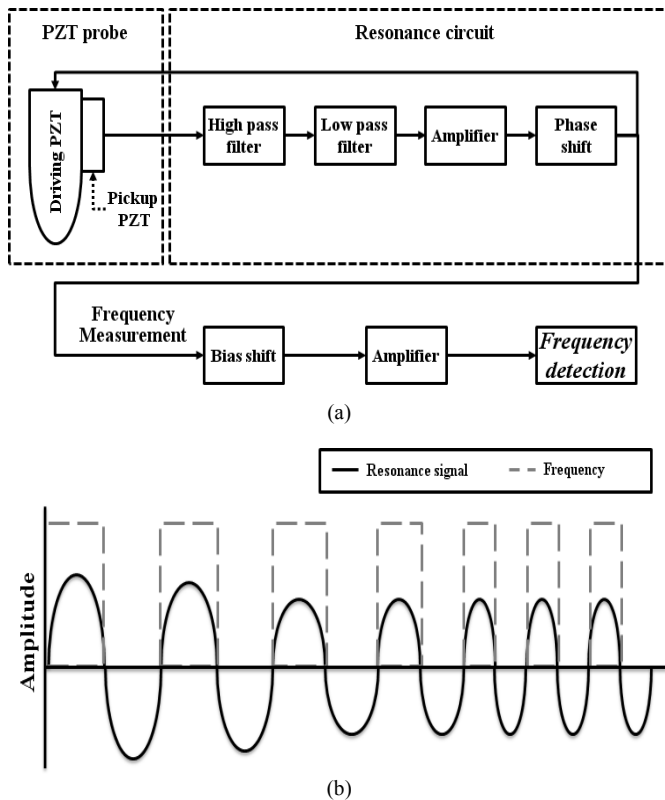


Fig. 1. (a) Block diagram of the resonance circuit for aMSS and (b) aMSS output signals: resonance signal, and conversion signals for frequency

III. METHODS

The aMSS measures the muscle contraction based on the resonance signal changes, and the signal is driven from a piezoelectric transducer (PZT). The resonating PZT probe consists of two parts: PZT probe and resonance circuit, shown in Fig.1 (a). The probe is designed by combining a driving PZT with a pickup PZT. The driving PZT (PSt 150/5x5/7, *PIEZOMECHANIC*, DE) causes mechanical vibration and the pickup PZT (PSt 150/2x3/5, *PIEZOMECHANIC*, DE) measures the vibration. The size of the pickup PZT ($2 \times 3 \times 5 \text{ mm}^3$) is smaller than that of the driving PZT ($5 \times 5 \times 7 \text{ mm}^3$) in order to reduce the effect from the PZT mass and resonance frequency. The resonance circuit produces a stable periodic signal for the PZT probe. The resonance circuit consists of amplifier, filter and phase compensator. Because the raw signal acquired from the pickup PZT has insufficient power to drive the probe, it should be amplified for resonance. The raw signal is amplified with a gain of two, and filtered with a band pass filter (f_{cutoff} : 100 - 150 kHz) to extract only the resonance frequency according to frequency response of the aMSS. The amplifier and filter distort the signal phase; the distorted phase is compensated with a phase shift circuit.

The frequency-reflected signal is measured from the resonance signal. Fig.1 (b) shows the relationship between the signals conceptually. The frequency-reflected signal is then altered to a binary signal, a dashed line in Fig.1 (b), from the resonance signal, solid line. The binary signal, 0 and 5 volts,

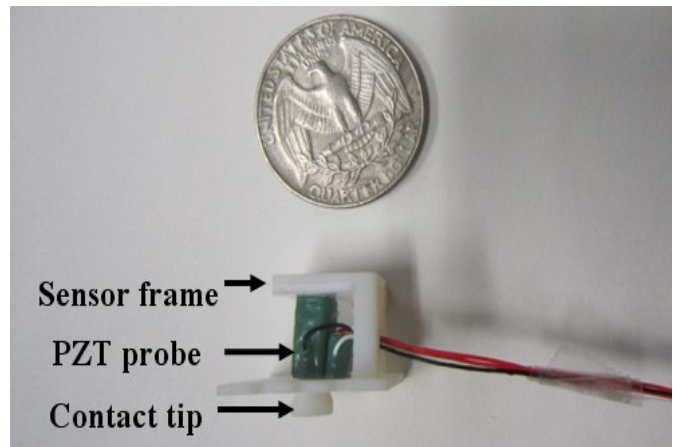


Fig. 2. aMSS components; resonating PZT probe, sensor frame, and contact tip

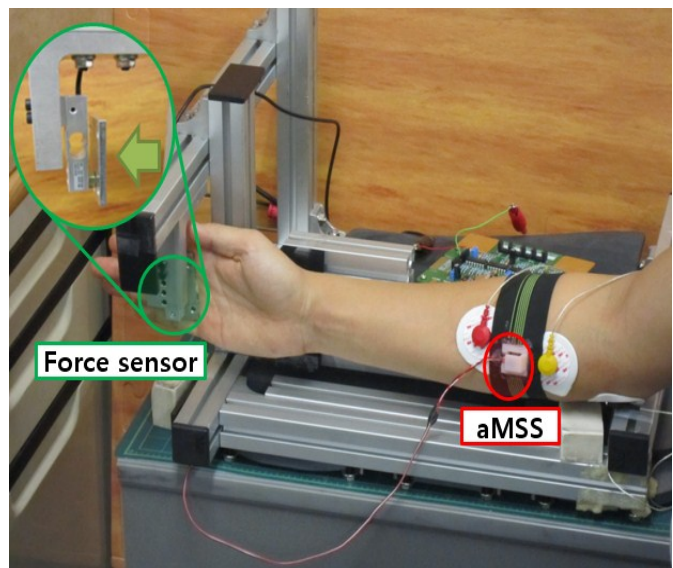
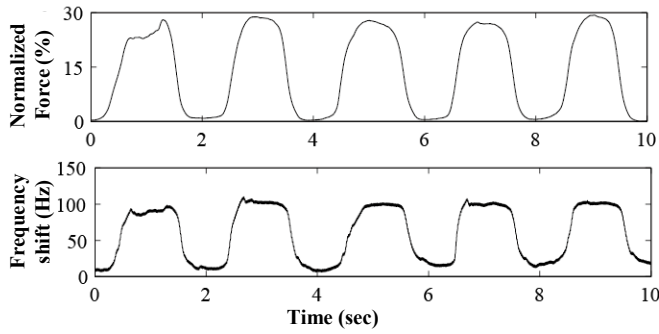


Fig. 3. Experimental setup: aMSS, and force sensor

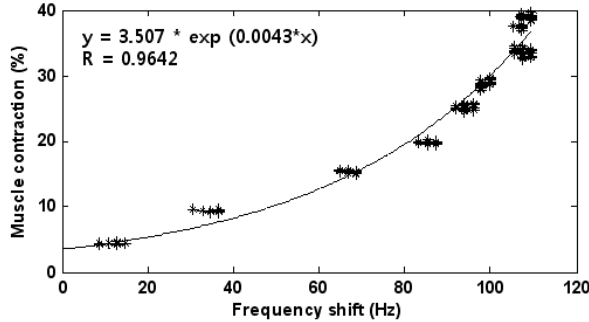
maintains constant amplitude for frequency counter despite of the resonance signal amplitude change.

IV. EXPERIMENTAL SETUP

The sensor performances are evaluated by comparing the muscle contraction in accuracy aspect. A force sensor is used for comparison of each performance. The target motion is wrist flexion, and we measure a flexor carpi radialis (FCR), one of major responsible muscle for wrist flexion and located close to skin. The muscle is measured in isometric condition in which the muscles contract without any appreciable joint movement or muscle length change. A test device is designed to keep the isometric wrist flexion and described in Fig.3. The forearm, wrist, and elbow are fixed to the device, and the upper arm keeps the position vertically to the forearm for the isometric contraction of the FCR. The force sensor is located on a palm of the hand to measure the wrist flexion force. The sensor is located on a belly of the FCR. The sensor outputs are acquired by a digital acquisition board (NI PCI-6251,



(a)



(b)

Fig. 4. (a) Voluntary isometric contraction: resonance frequency shift of aMSS, amplitude change of aMSS, sEMG, and muscle contraction (b) Contraction test: resonance frequency shift of aMSS and amplitude change of aMSS in proportion to muscle contraction

National Instrument, US) and its software (Labview6.2, National Instrument, US). All of the signals are acquired with 1 kHz sampling frequency.

Eight healthy subjects (22 to 41 years old) are recruited in the experiment. Before the tests, the maximal voluntary contraction (MVC) of the subjects was measured during the wrist flexion. Subjects applied contraction force, wrist flexion, to the fixed frame where the force sensor is attached, and they were demanded to flex their wrist in range of 0 to 40 % based on MVC for not in fatigue condition. Each of the force levels were repeated 5 times. Subjects followed the target forces that were displayed on the monitor.

V. RESULTS

A. Accuracy

The sensor measures the muscle contraction and compared them with the resultant force. Fig.4 (a) shows signals during the muscle contraction. The bottom figure is the muscle contraction based on the MVC from force sensor. The frequency shift has similar trends with the normalized force, and this means that the signal is highly correlated with the muscle contraction. The force level (F) are fit (\hat{F}) using an exponential function of the sensor signals as equation (2). Table I shows individual coefficients α and β according to ΔS

	AMPLITUDE CHANGE		
	MODELING		R^2
	α_{AS}	β_{AS}	
SUMMARY	0.648 ± 0.29	0.026 ± 0.011	0.957 ± 0.04

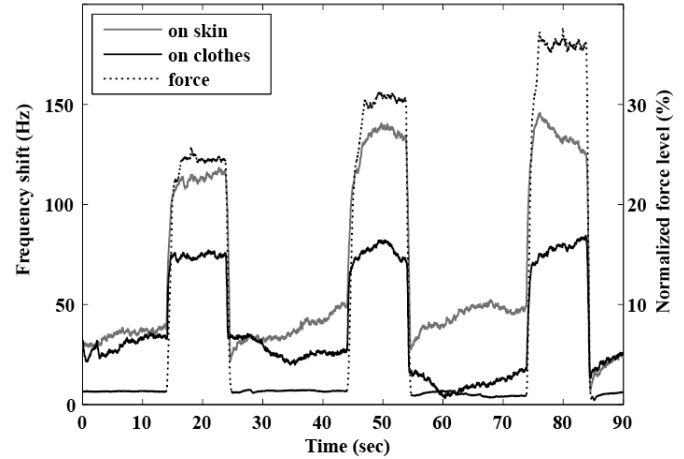


Fig. 5. aMSS amplitude change on skin and on clothes

as well as the coefficient of determination (R^2) between \hat{F} and the contraction level.

$$\hat{F} = \alpha_x \times \exp(\beta_x \times \Delta S) \quad (2)$$

The frequency shift measurement is proportional to the muscle contraction as described in Fig.4 (b) respectively. The signal is fitted exponentially to the muscle contraction and displayed on the graph. The correlation coefficient, R, is also displayed. The equation measure the muscle contraction with a high correlation, R= 0.964, and the average correlation coefficient of subjects is 0.957 \pm 0.04. The results mean that muscle contraction can be measured from the exponentially fitted sensor outputs.

B. Muscle contraction measurement on clothes

One advantage of the developed sensor is that it can measure the muscle contraction over clothes. The sensor can measure the muscle stiffness change through the cloth. The sensor is attached on the thin single-layer cotton shirt over the skin. Eight subjects who were already recruited in the previous test were recruited in this test. This test was repeated two times. In the first test, the muscle stiffness change was measured by the sensor directly in contact with the skin, which is the same condition as the previous test. The second test is proceeded that subjects wear their shirts and the sensor located over the cloth.

Fig.5 overlaps the output signals from both of the two tests; black line is output measured on the skin, and dotted line is output of the second test over the clothes. Both signals are

increased during the contraction, but their change ratios are quite different. When the amplitude of the signal measured directly from the skin changes to 80 Hz, one measured through the cloth changes to 40 Hz during 10 % muscle contraction in 10 to 20 sec. In 20 % contraction, signal measured from the skin changes to 100 Hz while signal measured through the cloth changes to 50 Hz. Overall, the amplitude of the signal through cloth is reduced 0.65 times compared with that of the signal on the skin.

The frequency shift reduction in signal through cloth is produced from the properties of the clothes. Stiffness and mass of the cloth affect the stiffness change of the sensor in contact with the muscle through the clothes. The clothes reduce the stiffness change, but still, the muscle stiffness change can be measured. The reduction ratio of the signal amplitude depends on the properties of the contact clothes. Although the changed ratio is reduced, the muscle stiffness change can be measured conveniently using the sensor without taking off the clothes.

VI. CONCLUSION

This paper introduces a novel real-time muscle contraction sensor. The sensor measures the contraction from the resonance signals, which are highly correlated with the contacted object stiffness. Additionally, the sensor is able to measure the contraction over clothes; this can be a strong advantage for motion estimation sensor. To analyze the sensor performance, the sensor was applied on the forearm under isometric contraction condition and measured the muscle contraction. As a result, the sensor showed high correlation between the sensor output and the generated force from muscle contraction. The correlation coefficient is higher than 0.91 and this result means that the sensor can be used for a muscle contraction sensor. The output of the sensor is similar to that of the force sensor, so the sensor can be used to measure the force more intuitively without any signal processing compared to sEMG and it is possible to use directly to a control input. This sensor also has the advantages in insensitivity on motion artifact due to much higher difference of frequency range, approximately a difference of four orders of magnitude.

The sensor still has some limitations. The active sensor should improve the power efficiency and construction progress. Also the sensor output has some variances. One possibility is the thickness of skin tissue, which lies between muscle and the sensor. If effect of the skin tissue thickness becomes larger, it becomes a multilayer viscoelastic problem, such as skin and muscle.

REFERENCES

[1] B. Dellon, Y. Matsuoka, Prosthetics, exoskeletons, and rehabilitation [Grand Challenges of Robotics], IEEE robotics & automation magazine 14 (2007) 30-34.

[2] Z. Bien, K. Park, J. Jung, J. Do, Intention reading is essential in human-friendly interfaces for the elderly and the handicapped, *Industrial Electronics, IEEE Transactions on* 52 (2005) 1500-1505.

[3] Y. N. T.Sato, J.Ichikawa, Y.Hatamura, and H.Mizoguchi, Active understanding of human intention by a robot through monitoring of human behavior, *IEEE/RSJ/GI International Conference on Intelligent Robot and Systems.*(1994) 405-414.

[4] D. G. L. Thomas S. Buchanan, Kurt Manal, and Thor F. Besier, Neuromusculoskeletal Modeling: Estimation of Muscle Forces and Joint Moments and Movements From Measurements of Neural Command, *J Appl Biomech* 20 (2004) 367-395.

[5] J. Moreno, L. Bueno , J. Pons, Wearable robot technologies, *Wearable robots: biomechatronic exoskeletons* (2008) 165.

[6] P. R. Cavanagh , P. V. Komi, Electromechanical delay in human skeletal muscle under concentric and eccentric contractions, *Eur J Appl Physiol Occup Physiol* 42 (1979) 159-63.

[7] R. W. Norman , P. V. Komi, Electromechanical delay in skeletal muscle under normal movement conditions, *Acta Physiol Scand* 106 (1979) 241-8.

[8] B. Rebsamen, C. Guan, H. Zhang, C. Wang, C. Teo, M. H. Ang Jr , E. Burdet, A Brain Controlled Wheelchair to Navigate in Familiar Environments, *Neural Systems and Rehabilitation Engineering.* (2010) 590-598

[9] C. J. D. Luca, The use of surface electromyography in biomechanics, *Journal of Applied Biomechanics* 13 (1997) 135-163.

[10] K. Kiguchi, K. Iwami, M. Yasuda, K. Watanabe , T. Fukuda, An exoskeletal robot for human shoulder joint motion assist, *Mechatronics, IEEE/ASME Transactions on* 8 (2003) 125-135.

[11] C. Orizio, D. Liberati, C. Locatelli, D. De Grandis , A. Veicsteinas, Surface mechanomyogram reflects muscle fibres twitches summation, *Journal of biomechanics* 29 (1996) 475-481.

[12] W. Youn , J. Kim, Estimation of elbow flexion force during isometric muscle contraction from mechanomyography and electromyography, *Medical and Biological Engineering and Computing* (2010) 1-9.

[13] A. Chianura , M. E. Giardini, An electrooptical muscle contraction sensor, *Med Biol Eng Comput* 48 (2010) 731-4.

[14] T. Deffieux, J. L. Gennisson, M. Tanter, M. Fink , A. Nordez, Ultrafast imaging of in vivo muscle contraction using ultrasound, *Applied physics letters* 89 (2006) 184107.

[15] N. Vanello, V. Hartwig, M. Tesconi, E. Ricciardi, A. Tognetti, G. Zupone, R. Gassert, D. Chapuis, N. Sgambelluri , E. P. Scilingo, Sensing glove for brain studies: Design and assessment of its compatibility for fMRI with a robust test, *Mechatronics, IEEE/ASME Transactions on* 13 (2008) 345-354.

[16] F. H. P. Lukowicz, C. Szubski, and W. Schobersberger, Detecting and interpreting muscle activity with wearable forece sensors, *LNCS* 3968 (2006) 101-116.

[17] L. P. Kenney, I. Lisitsa, P. Bowker, G. H. Heath , D. Howard, Dimensional change in muscle as a control signal for powered upper limb prostheses: a pilot study, *Med Eng Phys* 21 (1999) 589-97.

[18] K. Kong , D. Jeon, Design and control of an exoskeleton for the elderly and patients, *Mechatronics, IEEE/ASME Transactions on* 11 (2006) 428-432.

[19] S. Moromugi, S. Yoon, S. Kim, M. Tanaka, Y. Ohgiya, N. Matsuzaka , T. Ishimatsu, A training machine with dynamic load-control function based on muscle activity information, *Artificial Life and Robotics* 10 (2006) 126-130.

[20] C. Gubler-Hanna, J. Laskin, B. J. Marx , C. T. Leonard, Construct validity of myotonometric measurements of muscle compliance as a measure of strength, *Physiol Meas* 28 (2007) 913-24.

[21] S. Omata, Y. Murayama , C. Constantinou, Real time robotic tactile sensor system for the determination of the physical properties of biomaterials, *Sensors and Actuators A: Physical* 112 (2004) 278-285.

[22] R. Merletti , P. Parker, *Electromyography: Physiology, engineering, and noninvasive applications*, Wiley-IEEE Press, (2004)

[23] R. Lieber, *Skeletal muscle structure, function, and plasticity*, Wolters Kluwer Health/Lippincott Williams & Wilkins, (2002)